Available online at www.sciencedirect.com
SCIENCE DIRECT®
Nuclear Physics A 729 (2003) 787–808
NUCLEAR PHYSICS A
www.elsevier.com/locate/npe

Multi-photon exchange processes in ultraperipheral relativistic heavy-ion collisions

Gerhard Baur [a], Kai Hencken [b,*], Andreas Aste [b], Dirk Trautmann [b], Spencer R. Klein [c]

[a] *Forschungszentrum Jülich, 52425 Jülich, Germany*
[b] *Universität Basel, 4056 Basel, Switzerland*
[c] *Lawrence Berkeley National Laboratory, Berkeley, CA 94720, USA*

Received 16 July 2003; received in revised form 9 September 2003; accepted 11 September 2003

Abstract

The very strong electromagnetic fields present in ultraperipheral relativistic heavy-ion collisions lead to important higher-order effects of the electromagnetic interaction. These multi-photon exchange processes are studied using perturbation theory and the sudden or Glauber approximation. In many important cases, the multi-photon amplitudes factorize into independent single-photon amplitudes. These amplitudes have a common impact parameter vector, which induces correlations between the amplitudes. Impact-parameter dependent equivalent-photon spectra for simultaneous excitation are calculated, as well as, impact-parameter dependent $\gamma\gamma$-luminosities. Excitations, like the multi-phonon giant dipole resonances, vector meson production and multiple e^+e^--pair production can be treated analytically in a bosonic model, analogous to the emission of soft photons in QED.

1. Introduction

In ultraperipheral relativistic heavy-ion collisions (UPC) very strong electromagnetic fields are present for a very short time [1]. The parameter which characterizes the strength of the interaction is the Coulomb parameter η:

* Corresponding author.
E-mail address: k.hencken@unibas.ch (K. Hencken).

0375-9474/$ – see front matter
doi:10.1016/j.nuclphysa.2003.09.006

$$\eta = \frac{Z_1 Z_2 e^2}{\hbar v} \approx Z_1 Z_2 \alpha, \tag{1}$$

where Z_1 and Z_2 are the charges of the nuclei and $v \approx c$ is the relative velocity of the ions. For heavy nuclei like Au–Au (RHIC) or Pb–Pb (LHC) $\eta \gg 1$. One can treat these systems semiclassically, with the nuclei following classical Rutherford trajectories. At high energies they are well approximated by straight lines with impact parameter b. In addition to elastic scattering, which is due to the exchange of many photons, there are various kinds of inelastic processes, like nuclear excitations, photon–nucleus interactions leading to baryonic or mesonic excitations and photon–photon processes. One can calculate the amplitudes for these processes in the same way as the corresponding ones for real photons [2,3].

Probabilities for the excitation of the giant dipole resonance (GDR) and e^+e^--pair production are very large, of the order of one for small impact parameter [2]. This means that these processes will also occur simultaneously with other interesting processes, where the probabilities are generally much smaller than one. The GDR is a strongly collective mode in nuclei. The theory of relativistic heavy-ion excitation of one- and multi-phonon GDR states is given in [4]. There is also mutual excitation, where each ion is excited to the (one phonon) GDR state. This process has been recently studied experimentally at RHIC [5]; it is important for the luminosity determination and for triggering on UPCs [6,7]. The fact that the double phonon giant dipole resonance is excited strongly in a two-photon excitation mechanism is of special interest for nuclear structure physics. The properties of these new collective modes could be explored with this method [8].

The probability of electron–positron pair production calculated in lowest-order perturbation theory exceeds the unitarity limit of one [9–11]. This means that multiple e^+e^--pair production is expected to be appreciable for heavy ions at RHIC and LHC conditions.

The probability $P(b)$ of other inelastic processes is in general much smaller than one. An important process is diffractive vector meson production (especially ρ^0-production). Probabilities for ρ^0-production in close (grazing) collisions are about 0.01 or 0.03 for RHIC and the LHC, respectively. The probability of the multiple (double) electromagnetic production of ρ^0 mesons is of the order of 10^{-3} to 10^{-4} [12].

One example of simultaneous processes is giant dipole resonance excitation (followed by neutron decay) accompanied by ρ^0-production. This process was recently studied experimentally at STAR [7].

This paper will present a general, unified treatment of multi-photon processes in heavy-ion collisions, focusing on the correlations which occur because all of the processes share a common impact parameter, $\vec{b}$. Section 2 reviews the semiclassical treatment and then introduces multi-photon interactions. Section 3 presents some examples of multi-photon processes and gives examples of the correlations, with RHIC and the LHC used for illustration. We give our conclusions in Section 4. A preliminary account of part of the present work is given in Ref. [13].

2. Theory

We work in the rest frame of one of the nuclei ("target system"). The other nucleus moves on a straight line with impact parameter $b > R_1 + R_2$ (where the nuclear radii are

R_1 and R_2, respectively). The corresponding Lorentz-factor is $\gamma = 1/\sqrt{1 - v^2/c^2}$. It is related to the Lorentz-factor $\gamma_{\rm coll}$ in the collider frame by $\gamma = 2\gamma_{\rm coll}^2 - 1$.

Since the strength of the electromagnetic interaction decreases with increasing impact parameter b, the excitation probability also decreases, in many important cases proportional to $1/b^2$. Higher-order effects are proportional to the product of such probabilities, and are therefore especially important for collisions with impact parameter b close to $b_{\rm min} = R_1 + R_2$.

The collision time is given by $\tau_{\rm coll} = b/\gamma$, so the electromagnetic spectrum will include frequencies up to

$$\omega_{\rm max} \approx \frac{\gamma}{b_{\rm min}}. \tag{2}$$

2.1. Elastic Coulomb collisions

A simple and rather accurate result is well known for classical Coulomb scattering at small angles $\theta \ll 1$ [14]. The momentum transfer is

$$\Delta p = \frac{2Z_1 Z_2 e^2}{bv} = \frac{2\eta\hbar}{b} \tag{3}$$

in the direction perpendicular to the motion. The momentum transfer is related to the scattering angle θ by $\Delta p \approx p\theta$. From this classical relation between the impact parameter and the scattering angle one can calculate the classical relativistic Rutherford scattering cross-section as

$$\frac{d\sigma}{d\Omega} = \left[\frac{2Z_1 Z_2 e^2}{pv}\right]^2 \frac{1}{\theta^4}, \tag{4}$$

where $p = \gamma M_1 v$ and M_1 is the mass of nucleus Z_1, see, e.g., p. 644 of [14]. This result can also be obtained in a field theoretical approach, which we only sketch here. Coulomb scattering is due to the exchange of photons. The sum over all the ladders diagrams, crossed and uncrossed, can be done in the high-energy limit and for forward angles [15–17]. A typical diagram is shown in Fig. 1(b).

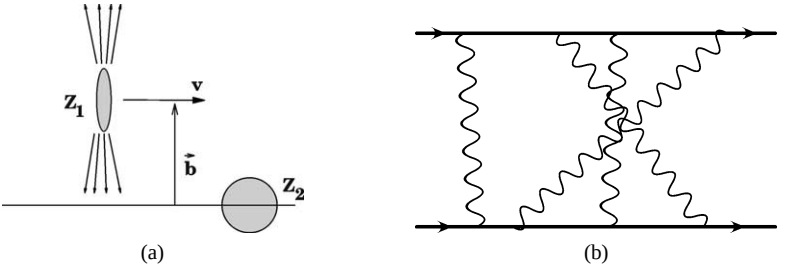

(a) (b)

Fig. 1. (a) Classical picture of heavy-ion scattering. This picture was also used by Fermi in his celebrated paper on the equivalent photon approximation [18]. He considered the non-relativistic case $v \ll c$. The relativistic case is discussed in a very pedagogical manner in [14]. (b) For $\eta \gg 1$ many photons are exchanged in elastic heavy-ion scattering. A typical graph is shown.

One ingredient in this procedure is the linearization of the propagator denominator

$$\frac{1}{(p+q)^2-m^2} \approx \frac{1}{2p\cdot q}. \tag{5}$$

In order to sum up all ladder and crossed ladder graphs one uses the identity

$$\sum_{\sigma} \frac{1}{a_{\sigma(1)}(a_{\sigma(1)}+a_{\sigma(2)})\cdots(a_{\sigma(1)}+a_{\sigma(2)}+\cdots+a_{\sigma(n)})} = \frac{1}{a_1 a_2 \cdots a_n}, \tag{6}$$

where the sum is over all permutations σ of the indices 1 to n.

Summing over all orders the scattering amplitude is found similar to the eikonal approximation in (non-relativistic) potential scattering:

$$f_{\rm el}(q) = \frac{p}{2\pi i}\int d^2b \exp(i\vec{q}\cdot\vec{b})\big[\exp\big(i\chi(b)\big)-1\big]. \tag{7}$$

By integrating over the angle ϕ

$$f_{\rm el}(q) = ip\int_0^\infty db\, bJ_0(qb)\big[1-\exp\big(i\chi(b)\big)\big]. \tag{8}$$

In this approach there is a well defined momentum transfer $q=\Delta p$ (we set $\hbar=1$), and the impact parameter b is not an observable quantity. For the elastic Glauber phase $\chi(b)$ in the case of photon exchange, the analytic expression is well known, see, e.g., [19]:

$$\chi(b) = -2\eta K_0(\lambda b), \tag{9}$$

where λ is a small photon mass needed to regularize the integral at large b.

For $\eta \gg 1$ the integrand oscillates very rapidly and large contributions to the integral are only obtained when the phase of this integrand is stationary. One can introduce the saddle point ("stationary phase") approximation [20]

$$\int e^{i\Phi(t)}\,dt \approx e^{i\Phi(t_0)}\sqrt{\frac{2\pi i}{\Phi''(t_0)}}, \tag{10}$$

where t_0 is determined by $\Phi'(t_0)=0$. (One may have to sum over various stationary points t_0.) In our case we have a two-dimensional integration over $\vec{b}$; for a derivation of the semiclassical case using only a one-dimensional saddle point approximation, see [21]. Assuming that the momentum transfer $\vec{q}$ points in the x-direction, the phase in the integrand of Eq. (7) is (for small λ)

$$\Phi(\vec{b}) = q_x b_x + 2\eta\ln(\lambda b). \tag{11}$$

The conditions

$$\frac{\partial\Phi}{\partial b_y} = 2\eta\frac{b_y}{b^2} = 0, \qquad \frac{\partial\Phi}{\partial b_x} = q_x + 2\eta\frac{b_x}{b^2} = 0 \tag{12}$$

lead on the one hand to $b_y=0$, that is the dominant contribution comes from the direction, where $\vec{b}$ is parallel to $\vec{q}$. It also leads to an extremum for $b_x=-b_0$ with

$$q=\Delta p = \frac{2\eta}{b_0}, \quad b_0 = \frac{2\eta}{q}. \tag{13}$$

The second derivatives at the saddle point are

$$\frac{\partial^2 \Phi}{\partial b_x^2} = \frac{-2\eta}{b_0^2}, \qquad \frac{\partial^2 \Phi}{\partial b_x \partial b_y} = 0, \qquad \frac{\partial^2 \Phi}{\partial b_y^2} = \frac{2\eta}{b_0^2}. \tag{14}$$

Therefore an approximation of the elastic scattering amplitude up to a phase is

$$\left| f_{\rm el}(q) \right| = \frac{p b_0^2}{2\eta} = \frac{2p\eta}{q^2}, \tag{15}$$

giving the same cross-section as the classical calculation.

Eq. (13) gives the classical connection of the momentum transfer q to the impact parameter b_0, see above Eq. (3). The dominant contribution to the (pseudo-)Gaussian integral comes from values of $\vec{b}$ around the classical impact parameter b_0 in (opposite) direction of $\vec{q}$, with a width ("uncertainty of the b-value", see Eq. (14)) of $b_0/\sqrt{\eta}$.

The classical momentum transfer Δp is built up from the perpendicular momenta of many exchanged photons. The perpendicular momentum of the individual photon is restricted to $q_\perp \lesssim 1/b$, so 2η photons must be exchanged to reach the classical Δp. This contrasts with electron or proton scattering, where $\eta = 1/137 \ll 1$ for $v \approx c$. So, in the following, we use the semiclassical approximation to describe inelastic processes in the case $\eta \gg 1$.

For $b < R_1 + R_2$ one has to consider strong interactions. In many cases, especially for heavy ions, the "black disk approximation" is quite good. In this approximation χ is very large and imaginary for $b < R_1 + R_2$. In the case of strong Coulomb elastic scattering ($\eta \gg 1$), including the strong absorption of the ions for $b < R_1 + R_2$, the diffraction pattern is given by Fresnel diffraction (rather than a Fraunhofer one for $\eta < 1$). This is explained in detail in [22], see also Section 5.3.5 of [23]. These grazing angles are extremely small, about 5×10^{-5} (rad) for Au–Au collisions RHIC and 2×10^{-6} (rad) for Pb–Pb collisions at LHC (in the collider frame); they are well below the beam emittance, so the scattered ions will remain in the beam. Although the previous discussion is not entirely new, we think that it is useful to present the general ideas, which relate classical and quantal (or field-theoretical) descriptions of scattering in strong Coulomb fields, which may be a rather unfamiliar subject.

2.2. Perturbation theory for inelastic processes

In the following we use the semiclassical approximation and treat the Coulomb field of the ion(s) as classical external fields. One ion moves on a straight line trajectory with a definite impact parameter, while the other ion is at rest. The semiclassical approximation can be justified in the same way as in the elastic case. The scattering amplitude in the inelastic case is given in the eikonal approximation by [21]

$$f_{\rm fi}(\vec{q}) = \frac{p}{2\pi i} \int_0^\infty d^2 b \exp(i\vec{q} \cdot \vec{b}) \exp\bigl[i\chi(b)\bigr] a_{\rm fi}(\vec{b}). \tag{16}$$

The amplitude $a_{\rm fi}$ can be expanded in the form $a_{\rm fi}(\vec{b}) = \sum_\mu a_{\rm fi}^\mu(b)\exp(i\mu\phi)$ where μ denotes the angular momentum transfer along the beam axis. After integration over the azimuthal angle ϕ,

$$f_{\rm fi}(\vec{q}) = -ip\int_0^\infty db\sum_\mu J_\mu(qb)i^\mu\exp\bigl[i\chi(b)\bigr]a_{\rm fi}^\mu(b). \tag{17}$$

Using the saddle point approximation, the connection to the semiclassical case can clearly be seen and $a_{\rm fi}(\vec{b})$ corresponds to the semiclassical excitation amplitude. In the semiclassical approximation, the scattering amplitude is the product of the elastic Coulomb scattering amplitude and the semiclassical excitation amplitude $a_{\rm fi}(b)$. We have

$$f_{\rm fi}(\vec{q}) = f_{\rm el}(q)a_{\rm fi}(-b_0\hat{q}) = f_{\rm el}(q)\sum_\mu(-1)^\mu a_{\rm fi}^\mu(b_0), \tag{18}$$

where $\hat{q}$ is the unit vector pointing in the $\vec{q}$-direction (see Eqs. (11)–(14)). While we have not made numerical comparisons of the field theoretic solution to the semiclassical approximation in the relativistic case, such comparisons exist for the non-relativistic electromagnetic excitation. In this case the electromagnetic cross-sections can be calculated exactly. They depend essentially on the Coulomb parameter η which approaches infinity in the semiclassical approximation. It is found (see, e.g., Fig. (II.9) of [24]) that the asymptotic (semiclassical) limit is reached already for rather low η values. The semiclassical approximation works better than one may expect. In Au–Au or Pb–Pb collisions $\eta \approx 50$, so the semiclassical approximation should be excellent.

The electric charge of the relativistic ion gives rise to an electromagnetic potential, the Lienard–Wiechert potential $A_\mu(\vec{r},t)$

$$\begin{aligned} A_0(\vec{r},t) &= \phi(\vec{r},t) = \frac{Z_p e\gamma}{\sqrt{(b-x)^2+y^2+\gamma^2(z-vt)^2}}, \\ \vec{A}(\vec{r},t) &= \frac{\vec{v}}{c}\phi(\vec{r},t). \end{aligned} \tag{19}$$

The interaction with the target is described in terms of an electromagnetic current operator $\hat{j}_\mu$. This leads to a time-dependent electromagnetic interaction of the form

$$V(t) = \int d^3r\, A_\mu(\vec{r},t)\hat{j}^\mu(\vec{r}). \tag{20}$$

The dependence of $V(t)$ on the impact parameter is not shown explicitly. The target current $\hat{j}_\mu$ describes a wealth of physics and is a quite complicated object in general. This current contains the current of the nucleus and the interaction leads to the excitation of nuclear states, with the giant dipole resonance (GDR) as an important example. It also describes photonuclear interactions like nucleon excitations, meson production and photon–photon interactions, for example, lepton pair production. The lepton (e^+e^-) states are those in the external Coulomb field of the target, i.e., the Furry picture is used here. Now one can expand the (time dependent) target state $\Phi(t)$ in terms of all possible states Φ_n which can be reached by the interaction $V(t)$. We write

$$\Phi(t) = \sum_n a_n(t)\exp(-iE_nt)\Phi_n, \tag{21}$$

where we have introduced the time-dependent amplitudes $a_n(t)$ for the state Φ_n. The (time-independent) states Φ_n consist of all states which can be connected to the target nucleus ground state by the interaction V (i.e., due to the interaction with the (virtual) photons). This includes, for example, excited nuclear states, the nucleus in its ground state and lepton pairs, or mesons, or nuclear excited states along with lepton pairs, or mesons, etc.

One can set up coupled equations for the amplitudes $a_n(t)$ [25]. They are

$$i\dot{a}_n = \sum_m \langle n|V(t)|m\rangle \exp\bigl(i(E_n - E_m)t\bigr)a_m(t). \tag{22}$$

The initial condition is $a_m(t \to -\infty) = \delta_{m0}$. The expression on the r.h.s. can be viewed as the matrix element of the operator

$$\tilde{V}(t) = \exp(iH_0t)V(t)\exp(-iH_0t) \tag{23}$$

("interaction representation"). A formal solution of this equation can be written down using the time-ordering operator $\mathbb{T}$:

$$a_n(t \to +\infty) = \langle n|\mathbb{T}\exp\left(-i\int_{-\infty}^{+\infty} dt\ \tilde{V}(t)\right)|0\rangle. \tag{24}$$

We use perturbation theory to solve this equation. Since the electromagnetic interaction V is in general weak, this is a good procedure. The first-order amplitude is

$$a_n^{(1)} = -i\int_{-\infty}^{\infty} dt\ V_{n0}(t)\exp(i\omega_{n0}t), \tag{25}$$

where $V_{nm}(t) = \langle n|V(t)|m\rangle$ and $\omega_{nm} = E_n - E_m$. This is the one-photon approximation. In second order

$$a_n^{(2)} = \frac{1}{i^2}\sum_m \int_{-\infty}^{\infty} dt\ V_{nm}(t)\exp(i\omega_{nm}t)\int_{-\infty}^{t} dt'\ V_{m0}(t')\exp(i\omega_{m0}t'), \tag{26}$$

where the sum is over all intermediate states m. Only if the integrand is symmetric in t and t' one can extend the integral over t' to infinity and factorize the amplitude. This is not possible here since the operator $\tilde{V}$ does not commute in general for different times t and t'. (In the case of the excitation of a harmonic oscillator, the commutator of these operators is a c-number and a full analytical solution can be found; this case will be treated below in Section 2.4.)

In the case of the excitation of two independent modes, that is of two modes which do not mix with each other since their interaction is zero or negligible, there is such a factorization: let us assume that one excites a state $n = (\alpha, \beta)$ where α denotes, e.g., a nuclear excited state and β a vector meson in a state with a given momentum and helicity produced coherently. Two types of intermediate states contribute to the sum over m, see Fig. 2, $m = (0, \beta)$ and $m = (\alpha, 0)$. By summing over them the integrand becomes symmetric in t and t'. Formally this can then be written in the following way: the first path goes from the state $0 = (0, 0)$ to $(\alpha, 0)$ and then to (α, β). The contribution of this path to

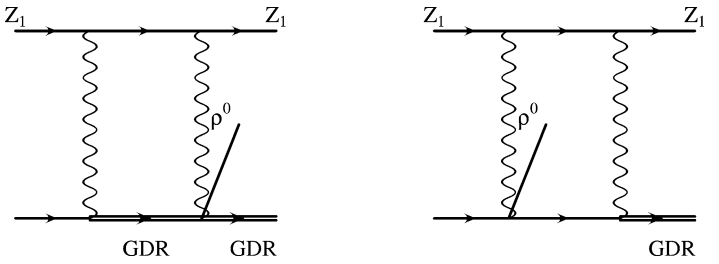

Fig. 2. Graphs contributing to the simultaneous excitation of states α and β. In this figure we take $\alpha = \text{GDR}$ and $\beta = \rho^0$ as a typical example.

the second-order matrix element is

$$a^{(2)}_{(\alpha,\beta)}(1) = \frac{1}{i^2}\int_{-\infty}^{\infty} dt\, V_{(\alpha,\beta)(\alpha,0)}(t)\exp(i\omega_{\beta 0}t) \times \int_{-\infty}^{t} dt'\, V_{(\alpha,0)(0,0)}(t')\exp(i\omega_{\alpha 0}t'), \tag{27}$$

and for the second path

$$a^{(2)}_{(\alpha,\beta)}(2) = \frac{1}{i^2}\int_{-\infty}^{\infty} dt\, V_{(\alpha,\beta)(0,\beta)}(t)\exp(i\omega_{\alpha 0}t) \times \int_{-\infty}^{t} dt'\, V_{(0,\beta)(0,0)}(t')\exp(i\omega_{\beta 0}t'). \tag{28}$$

The independence of the two processes corresponds to the assumption that the presence of the state α (or β) does not influence the interaction matrix element for the production of β (or α) (and that a single photon cannot produce a single step transition from $(0, 0)$ to (α, β), see below):

$$V_{(\alpha,\beta)(0,\beta)} = V_{(\alpha,0)(0,0)} = V_{\alpha 0}$$

and

$$V_{(\alpha,\beta)(\alpha,0)} = V_{(0,\beta)(0,0)} = V_{\beta 0}.$$

In many important practical cases this independence should be very well fulfilled. For mutual excitation the factorization is well understood, the elastic form factor of the excited ion is almost unchanged from the one of the ion in its ground state. Even the slight change in form factor takes time, as will be discussed below in connection with the validity of the sudden limit.

Similarly for photon–photon processes like lepton-pair production together with nuclear excitation, the photon–photon process depends only on the charge of the nucleus, with little sensitivity to the details of the charge distribution. The nucleus is not influenced

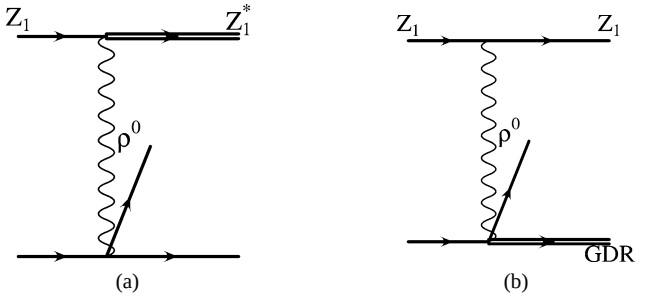

Fig. 3. Examples of graphs which spoil the factorization of the different processes, compare also with the figure above. As discussed in the text their contribution are expected to be small.

by the additional photon–photon process and vice versa. For hadronic final states, where there may be strong interactions with the nuclei, the photon–photon process in a double equivalent photon approach will predominantly occur outside the two nuclei.

Adding the amplitudes of the two paths, Eqs. (27) and (28) one can see that the integrand is symmetric in t and t' and one obtains factorization. In an obvious way this is generalized to the excitation of N independent modes. For any function $f(t_1, t_2, \ldots, t_n)$ which is symmetric in all variables t_i

$$\int_{-\infty}^{t} dt_1 \cdots \int_{-\infty}^{t} dt_n \, f(t_1, \ldots, t_n) = n! \int_{-\infty}^{t} dt_1 \int_{-\infty}^{t_1} dt_2 \cdots \int_{-\infty}^{t_{n-1}} dt_n \, f(t_1, t_2, \ldots, t_n). \tag{29}$$

One can use this formula to factorize the amplitude into a product of first-order amplitudes. The factor of $1/n!$ is compensated by the $n!$ different ways to order the excitation of the independent modes $\alpha, \beta, \gamma, \ldots$.

Let us give here also an example of two modes, which are coupled (i.e., no longer independent): the excitation of vibrational and rotational modes of a nucleus [26]. These modes mix due to rotation–vibration coupling. This gives rise to nuclear eigenstates of a mixed character. In the case of ρ^0 production and GDR excitation, for example, such a coupling is expected to be so small that it can safely be neglected.

The factorization is also not fulfilled in single photon exchange processes, which are depicted in Fig. 3. One such process is photon exchange with inelastic vertices on both sides (Fig. 3(a)). This process was studied in [27,28] within an inelastic EPA approach and was found to be only of the order of 1% as compared to the elastic process. Another example is the GDR excitation together with the meson production, see Fig. 3(b). This is a special contribution to the incoherent meson production process. Again this process is expected to be small: the vector meson is mainly produced through a diffractive (absorptive) process, which is very ineffective for a GDR excitation. The magnitude of such a process could be estimated by looking, e.g., at the GDR excitation in inelastic meson

scattering at high energies. Unfortunately we are unaware of any study that has been done at these high energies.

Asymmetric systems, such as d–A are also of interest, as shown by the recent d–Au run at RHIC, where UPCs were studied [29]. In these collisions, non-factorizable processes could come into play. The Coulomb parameter is $\eta = 0.6$, less than one and the semiclassical approximation (used, i.e., in equations like Eqs. (3), (10) or (18)) does not apply. However, the total cross-sections (i.e., integrated over b and q, respectively) are equal in the semiclassical and Glauber (or plane wave) case [1,30]. In this run, the ρ^0+ nuclear breakup channel was studied. Due to the Z^2 dependence the photon(s) will come predominantly from the gold nucleus. The ρ^0+ breakup channel gets the main contribution from incoherent rho production, i.e., it is a one photon process of the form of Fig. 3(b). There is also a two-photon contribution from coherent ρ^0-production accompanied by an electromagnetic deuteron breakup [31]. This mechanism is suppressed by a factor of $P_{\text{breakup}}(b)$ relative to the incoherent one-photon mechanism, which is of the order of 1% in the relevant impact parameter range. Due to the selection mechanism in the experiment the incoherent rho meson production mechanism is disfavored. Therefore overall the balance between the two reaction mechanisms should be studied in more detail.

2.3. Multi-photon processes in the sudden or Glauber approximation

The solution of the coupled equations (22) is greatly facilitated if the sudden approximation can be applied, see, e.g., [30]. In this case the collision time $t_{\text{coll}} = b/\gamma$ is much smaller than the excitation time $1/\omega$. This condition is fulfilled in many interesting cases and we assume now that the sudden approximation can be used. This "frozen nucleus-"approximation is also used in Glauber theory. The relation between the semiclassical approach and the Glauber (or eikonal) approximation is explained in [30], for the non-relativistic, as well as, for the relativistic case. The excitation amplitude is

$$a_n(t \to \infty) = \langle n| \exp(i R)|0\rangle, \tag{30}$$

where

$$R = -\int_{-\infty}^{+\infty} dt\, V(t) = -\int_{-\infty}^{+\infty} dt\, A_\mu(t) \hat{j}^\mu. \tag{31}$$

The operator R is a direct sum of operators in the space of nuclear states, the space of the nucleus-vector meson system, the nucleus-e^+e^- system, etc. So,

$$R = \sum_i R_i, \tag{32}$$

where i denotes the different final states like e^+e^--pairs, ρ-mesons or a GDR excited ion. One has

$$\exp(i R) = \prod_i \exp(i R_i) \tag{33}$$

as the different R_i commute with each other. One may expand the exponential in Eq. (30). Terms linear in R describe, e.g., the excitation of nuclear states, like the collective

giant dipole resonance (GDR), vector meson production or e^+e^--pair production. Terms quadratic in R give, e.g., contributions to double-phonon GDR excitation, double vector meson production, double e^+e^--pair production. The quadratic terms also describe, e.g., vector meson production and GDR excitation in a single collision. A contribution to the second order amplitude $a^{(2)}$ is, e.g.,

$$a^{(2)} = -\langle \mathrm{GDR}|R|0\rangle\langle\rho^0|R|0\rangle, \tag{34}$$

where $|0\rangle$ denotes the ground state of the nucleus. In the general case the R_i commute and using Eq. (33) one gets

$$a = \langle \mathrm{GDR}|\exp(i\,R_{\mathrm{GDR}})|0\rangle\langle\rho^0|\exp(i\,R_{\rho 0})|0\rangle, \tag{35}$$

which has the second-order term as a special limit.

For three independent processes, say GDR excitation, vector meson- and e^+e^--pair production, the six different time orderings compensate for the $1/3!$ factor in the expansion of Eq. (30). In this formalism, processes are independent and the elementary amplitudes factorize, as one would have intuitively expected. This property is used also in the experimental analysis of vector meson production with simultaneous GDR excitation, where the neutrons from the GDR decay serve as a trigger on UPC [7]. The ion motion is not disturbed by the excitation process. The reason is that the kinetic energy of the ion is much larger than the excitation energy. Due to coherence, the quantity $x = \omega/E = 1/(RM_NA)$ is very small. One has $x < 4\times10^{-3}$, 3×10^{-4} and 1.4×10^{-4} for oxygen, tin and lead ions, respectively.

The GDR excitation immediately affects the nucleon momenta, but the nucleons will take a finite time to adjust their positions. With an excitation energy of about 20 MeV, the oscillation time of the GDR can be estimated classically to be about 10 fm/c. Due to the time dilatation, this corresponds to a time in the collider frame of about 1000 fm/c at RHIC and even longer at the LHC. This time is long compared to the time required to, for example, produce a ρ^0.

From the general discussion above of higher-order theory we have seen that this is not a necessary assumption to achieve factorization.

2.4. Excitation of a harmonic oscillator (bosonic modes)

An especially simple and important case is the excitation of a harmonic oscillator. It also has the virtue that it can be studied analytically. As some excitation processes in heavy-ion collisions can be regarded as quasibosonic processes, such a model can serve as a good approximation. Some examples are discussed below. Although well known (see, e.g., [32, 33]), we briefly present the main results of the excitation of a harmonic oscillator by an external force, this serves also to establish the notation.

In terms of the creation and destruction operators $a^\dagger$ and a the Hamiltonian of the system is

$$H = \omega\left(a^\dagger a + \frac{1}{2}\right), \tag{36}$$

where ω is the energy of the oscillator. The boson commutation rules are $[a, a^\dagger] = 1$ and $[a, a] = [a^\dagger, a^\dagger] = 0$. Only one mode is shown explicitly, in general one has to sum (integrate) over all the possible modes.

One assumes that the operator V (see Eq. (20)) is linear in the creation and destruction operators:

$$V(t) = f(t)a + f^*(t)a^\dagger. \tag{37}$$

In this case one can calculate $\tilde{V}$ explicitly using the boson commutation rules given above and the expansion

$$\tilde{V}(t) = V(t) + it\big[H_0, V(t)\big] + \frac{(it)^2}{2!}\big[H_0, \big[H_0, V(t)\big]\big] + \cdots. \tag{38}$$

One finds

$$\tilde{V}(t) = f(t)e^{-i\omega t}a + f^*(t)e^{i\omega t}a^\dagger. \tag{39}$$

Now one can convince oneself that the commutator of $\tilde{V}$ at different times t and t' is a pure c-number. In this case one can disregard the time ordering operator in Eq. (24) and obtain an exact analytical answer, up to an unimportant overall phase factor (see, e.g., [32]).

The excitation operator is the integral of the interaction over time

$$\int_{-\infty}^{+\infty} dt\, \tilde{V} = -(ua + u^*a^\dagger), \tag{40}$$

where u is the c-number

$$u = \int_{-\infty}^{\infty} dt\, f(t) \exp(-i\omega t). \tag{41}$$

This leads to the excitation of a so-called coherent state, see [34,35]. For the excitation of multi-phonon states this is explicitly shown in [36]. One has

$$a_n = \langle n|e^{-i(u^*a^\dagger + ua)}|0\rangle = \frac{(-iu^*)^n}{\sqrt{n!}}e^{-(1/2)uu^*}, \tag{42}$$

where the operator identity $e^{A+B} = e^A e^B e^{-(1/2)[A,B]}$ was used, which is valid for two operators A $(-iu^*a^\dagger)$ and B $(-iua)$ for which the commutator is a c-number. See also the discussion of the forced linear harmonic oscillator in [33].

Let us look at a few cases where this model can be applied: electromagnetic excitation of nuclear states, especially the collective giant multipole resonances was discussed recently by Bertulani [37]. The possibility to excite multi-phonon GDR states is studied in [38]. Multi-phonon GDR also play a role in the electromagnetic excitation of the ions in relativistic heavy-ion collisions, for a recent reference see [39,40]. The parameter which describes the probability $P_{\mathrm{GDR}}(b)$ of GDR excitation is (see [4])

$$P(b) = \frac{S}{b^2} \tag{43}$$

with a simple parameterization for S for the relevant high beam energies [1]

$$S = \frac{2\alpha^2 Z_1^2 N_2 Z_2}{A_2 m_N \omega} = 5.45 \times 10^{-5} Z_1^2 N_2 Z_2 A_2^{-2/3} \text{ fm}^2, \tag{44}$$

where m_N denotes the nucleon mass, and the neutron-, proton-, and mass-number of the excited nucleus are N_2, Z_2 and A_2, respectively. The excitation probability is inversely proportional to the energy ω (≈ 80 MeV$A^{-1/3}$) of the GDR state. As expected, the soft modes are more easily excited. Eq. (43) is based on the assumption that the classical dipole sum rule (Thomas–Reiche–Kuhn sum rule) is exhausted to 100%. For the excitation of an N-phonon state, a Poisson distribution is obtained. For heavy systems $P(b) \approx 1/2$ for close collisions ($b \gtrsim R_1 + R_2$).

Double ρ^0 production was studied in [12]. In addition to the label m for the magnetic substates of the GDR, there is a continuous label (the momenta). The probability to produce a ρ^0-meson in a close collision is of the order 1–3% for the heavy systems. It will be interesting to study these events experimentally to see how the ρ–ρ interaction affects the simple harmonic oscillator description, especially for the production of ρ^0's with close enough momenta.

Multiple e^+e^--pairs can be produced in relativistic heavy ion collisions [41]. This work used the sudden (or Glauber) approximation and a quasiboson approximation for e^+e^- pairs. Thus the Hamiltonian has the form of Eq. (36), where a sum over the quantum numbers of the lepton pair has to be included. Using a QED calculation (including Coulomb corrections in the Bethe–Maximon approach) for one pair production as an input, a Poisson distribution is obtained for multiple pair production. This is quite natural, since this problem reduces to the excitation of a harmonic oscillator (the modes are labelled by the spins and momenta of the e^+e^- pairs). More detailed calculations have verified that the Poisson distribution holds quite well for multiple pair production, although slight deviations are expected [2,10]. A characteristic dimensionless parameter for this problem is $\Xi = [(Z_1 Z_2 \alpha^2)^2]/(m_e b)^2$, where m_e is the electron mass and $b > 1/m_e$. Here, $\log \gamma$ should be large.

With heavy systems like Au–Au or Pb–Pb, when $b \gtrsim 1/m_e$, $\Xi \approx 1$. The impact parameter dependence of e^+e^--pair production has been studied numerically in lowest order QED [9]. Only recently an approximate analytical formula for the total pair production probability in lowest order $P^{(1)}$ was found. When $1/m_e < b < \gamma/m_e$ [42]

$$P^{(1)} = \frac{28}{9\pi^2} \Xi \left(2 \ln \gamma^2 - 3 \ln(m_e b)\right) \ln(m_e b). \tag{45}$$

The N-pair production probability decreases strongly with increasing impact parameter b (approximately like $\sim b^{-2N}$, for $b > 1/m_e$). Therefore the probabilities $P^{(1)}(b)$ should be known accurately for an impact parameter range of $0 < b <$ several $1/m_e$. Since the multiple pair production happens in a single collision, with a given impact parameter, there are correlations in the momenta of the outgoing pairs. This will be briefly discussed in Section 3 below.

e^+e^--pair production is of great practical interest. It could be useful as a trigger for UPC collisions at the LHC [43], but also constitutes a background for the most central parts of the trigger system of ALICE. [44]. Electron or muon pair production might also be a way to measure the $\gamma\gamma$-luminosity [45].

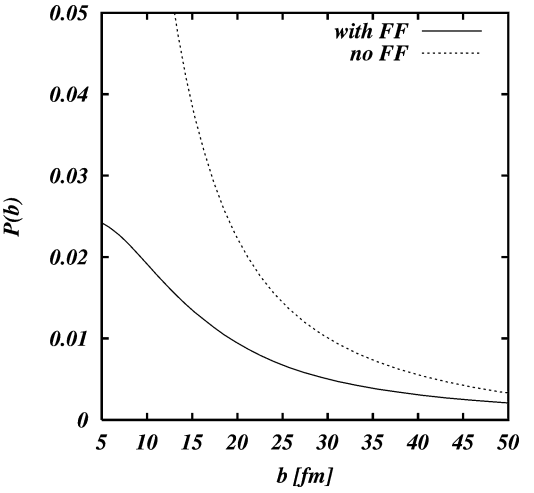

Fig. 4. The probability of muon pair production is shown as a function of impact parameter for Pb–Pb collisions at the LHC ($\gamma = 3400$). Results for a monopole form factor $F(Q) = 1/(1 + Q^2/\Lambda^2)$ with $\Lambda = 83$ MeV and without a form factor ($F(Q) = 1$) are given.

Muon pair production is also of interest: in close collisions the pair production probability is appreciable, although significantly smaller than one. This can be seen from Eq. (45). The muon Compton wavelength $1/m_\mu$ is 1.86 fm, much smaller than the nuclear radius. For $b \approx 2R_A$ form factor effects also need to be considered. Total cross-sections are smaller by about a factor of $(m_e/m_\mu)^2 \approx 2 \times 10^{-5}$ (which is still large). The results of a lowest order external field QED calculation are shown in Fig. 4. Calculations with and without a monopole form factor are shown. Details of the calculation are given in [10].

3. Some examples of multi-photon processes

The factorization of the amplitudes has some significant, experimentally accessible implications. Although the amplitudes are independent, the processes all share a common impact parameter $\vec{b}$. This leads to some significant correlations, due to both the magnitude and direction of $\vec{b}$. In this section, we consider the effect of multiple interactions on the photon spectrum and impact parameter distribution, and on the angular distributions of the final states.

3.1. Impact parameter dependence of the equivalent photon spectrum

The photon spectrum at impact parameter $b > R_A$ is

$$N(\omega, b) = \frac{Z^2\alpha}{\pi^2}\left(\frac{\omega}{\gamma}\right)^2\left(K_1^2(x) + \frac{K_0^2(x)}{\gamma^2}\right), \tag{46}$$

where $x = \omega b/\gamma$. As long as $x \ll 1$, the photon spectrum scales as $dN/d\omega \approx 1/b^2$. The mean impact parameter $\bar{b}$ is

$$\bar{b} = \frac{\int d^2b\, b\, P(b)}{\int d^2b\, P(b)}, \tag{47}$$

where the probability $P(b)$ of a specific reaction occurring at impact parameter b is

$$P(b) = N(\omega, b)\sigma_{\gamma A}. \tag{48}$$

For a reaction involving a single photon with energy ω, we can integrate over the region $b_{\min} = 2R_A < |b| < b_{\max} = \gamma/\omega$. Many processes can occur over a range of photon energies; in this case, an integral over ω is needed. However, the details of the interaction do not matter, and

$$\bar{b} = \frac{b_{\max} - b_{\min}}{\ln(b_{\max}/b_{\min})}. \tag{49}$$

For single photon processes the average impact parameter $\bar{b}$ is large when $b_{\max}$ is large and insensitive to the exact value of $b_{\min}$.

However, for two or more photon interactions, such as mutual Coulomb excitation of two nuclei, $P(b) \approx (d^2N_\gamma/d^2b)^n \approx 1/b^{2n}$, with n the number of photon interactions and the latter approximation requiring that the x for the two photons both be less than one. Then, as long as $b_{\max} \gg b_{\min}$,

$$\bar{b}_n \approx b_{\min}\frac{2n-2}{2n-3}. \tag{50}$$

$b_{\max}$ drops out, and the median impact parameter only depends on $b_{\min}$, independent of the collision energy and other details of the interaction. Of course, $b_{\max}$ depends on the photon energy and we assume that for all photon processes $b_{\max} \gg b_{\min}$ should be fulfilled in the relevant ω range. For heavy nuclei like Au $\bar{b}_2 \approx 2b_{\min} = 4R_A = 26$ fm.

For three-photon interactions, such as vector meson production accompanied by mutual Coulomb excitation of both nuclei, $n = 3$ and $\bar{b}_3 \approx 4b_{\min}/3 = 8R_A/3$. For heavy nuclei, $\bar{b}_3 \approx 18$ fm. Of course, as $\bar{b}_n$ drops with increasing n, the cross-sections for UPCs accompanied by hadronic interactions become more sensitive to the tails of the nuclear density profile—including these tails increases $b_{\min}$ above the canonical $2R_A$.

The $\bar{b}$ are comparable to the median impact parameters calculated in [46]; these detailed calculations found that the median impact parameter is almost independent of the specifics of the reaction. This impact parameter distribution is important for studying interference between vector meson production on the two nuclei; the smaller $\bar{b}$, the easier it is to observe the interference [47].

The reduction in $\bar{b}$ affects the photon spectrum, since the maximum photon energy scales as $1/b$. One way to quantify this is to consider a two-photon reaction: excitation of one nucleus to a GDR, while the second photon produces a ρ meson. The GDR tagging has a strong effect on the ρ^0-production: it selects small impact parameters, where the equivalent photon spectra are harder. One can calculate the equivalent photon spectrum in

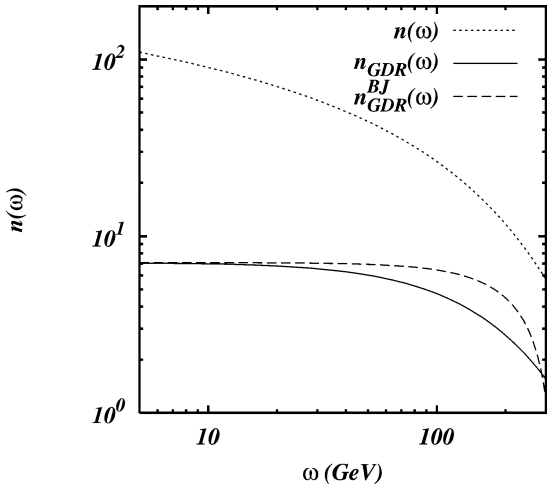

Fig. 5. The equivalent photon spectrum $n(\omega)$ (without tagging) is compared to the one for the excitation of a GDR resonance in one of the ions for Au–Au ($Z = 79$, $A = 197$) collisions at RHIC ($\gamma_{\rm coll} = 108$). The full expression is compared to the two approximations given in Eqs. (52) and (53).

the case of GDR tagging. For close collisions, which matter most, the probability of GDR excitation is given in Eqs. (43) and (44). The equivalent photon spectrum is then

$$n_{\rm GDR}(\omega) = S\frac{2Z_1^2\alpha}{\pi}\left(\frac{\omega}{\gamma v}\right)^2 \int\limits_{x_{\rm min}}^{\infty} \frac{dx}{x}\left(K_1(x)^2 + \frac{K_0(x)^2}{\gamma^2}\right). \tag{51}$$

This expression can be evaluated numerically. Due to the high values of the Lorentz boost γ at the colliders, $K_0(x)^2/\gamma^2$ is very small and can safely be neglected. A simple approximation [48] is found by setting $x^2K_1(x)^2 = 1$ for $x < 1$ and zero otherwise; the integral over x is then $1/(2x_{\rm min}^2) - 1/2$, where $x_{\rm min} = \omega R_{\rm min}/(\gamma v) < 1$. Then

$$n_{\rm GDR}^{\rm BJ}(\omega) \approx S\frac{Z_1^2\alpha}{\pi}\left(\frac{\omega}{\gamma v}\right)^2\left(\frac{1}{x_{\rm min}^2} - 1\right). \tag{52}$$

The photon spectrum scales very roughly as $n(\omega) \approx \omega^0$, in contrast to the $n(\omega) \approx \omega^{-1}$ for untagged photons.

Using Eq. (11.3.30) of Ref. [49] one finds a better analytic expression

$$n_{\rm GDR}(\omega) \approx \frac{S}{R_{\rm min}^2}\frac{Z_1^2\alpha}{\pi}x_{\rm min}^2\big(K_1(x_{\rm min})^2 - K_0(x_{\rm min})^2\big). \tag{53}$$

Fig. 5 shows the EPA spectrum $n(\omega)$ (without tag) and the spectrum $n_{\rm GDR}(\omega)$ in the approximations of Eqs. (52) and (53), respectively.

Another example of multi-photon processes is GDR tagging of $\gamma\gamma$-processes: if the mass of the system produced in the $\gamma\gamma$ interaction is low, there is a considerable influence of the tagging, if the mass is high, the influence is less. The b-dependence of (untagged) photon–photon processes can be found from the folding of b-dependent equivalent photon

spectra, see, e.g., Eq. (49) of Ref. [2]. A simple approximate formula was developed recently for the special case of e^+e^--pair production. The result is given in Eqs. (0.23), (0.16) and (0.17) of [42].

We consider here the more general case where the invariant mass of the $\gamma\gamma$-system is given by W (rather than $2m_e$, as in Ref. [42]). The lower cutoff in the impact parameter $b_{\min}$ is $2R_A$ (rather than the Compton wavelength $1/m$ of the electron). We introduce the parameters $u = b/R$ and $x = 2\gamma/(WR)$. We reconsider Eq. (0.24) of [42], with different integration limits: b_1 from R to b and ω_1 from $W^2R/4\gamma$ to γ/R. Generalizing Eqs. (0.16) and (0.17) of [42], the b-dependent $\gamma\gamma$-luminosity is

$$\frac{d^3L_{\gamma\gamma}}{d^2b\,dW} = \frac{2\pi}{WR^2}\left(\frac{Z^2\alpha}{\pi^2 u}\right)^2 X. \tag{54}$$

The probability $P_{AA}(b)$ of a $\gamma\gamma$-process in the AA collision is given in terms of this $\gamma\gamma$-luminosity by $P_{AA}(b) = 2\pi b\int(dW/W)(d^3L_{\gamma\gamma}/d^2b\,dW)\sigma_{\gamma\gamma}$. In this expression $\sigma_{\gamma\gamma}$ is the elementary $\gamma\gamma$ cross-section and

$$X = \left[\ln\left(\frac{x^2}{u}\right)\right]^2 \quad \text{for } x < u < x^2 \tag{55}$$

(for "large" impact parameters). For "small" impact parameters

$$X = 2\ln(u)\left(2\ln\left(\frac{x}{u}\right) + \frac{1}{2}\ln(u)\right) \quad \text{for } 2 < u < x. \tag{56}$$

This result is obtained by a generalization of Eq. (0.24) of [42].

The b-dependence is strongly influenced by the value of W: for $WR \ll \gamma$ (e.g., for low mass e^+e^- production) there is an approximate $1/b^2$-dependence over a considerable range of b-values, for $WR \approx \gamma$ the value of x is quite small and the dependence is much steeper. In this case low b-values are emphasized anyhow and the effect of tagging is less dramatic than for the case of ρ^0-production with GDR tagging, as discussed above. This was found by Klein in [50] for photon–photon processes with nuclear breakup. In accordance with the present considerations, the effect of tagging is more important for low W, see his plot as a function of the invariant mass of a produced muon pair $M_{\mu\mu}$. A comparison of the luminosity of Eq. (54) against a full calculation is shown in Fig. 6 for different invariant masses W. In view of the crude approximations made to obtain Eq. (54) the overall agreement is quite good for small invariant masses, whereas for the highest invariant masses shown in the plot some part of the cross-section come from the areas beyond the range $u < x^2$. This figure also shows the change in the shape of the spectrum for low and high invariant masses W.

3.2. Angular correlations

There can also be angular correlations since the photon polarization follows the electric field vector of the nuclear fields which in turn follows $\vec{b}$ [50]. For example, the decay $\rho_0 \to \pi^+\pi^-$ is sensitive to the photon polarization, and hence to the direction of $\vec{b}$. Mutual

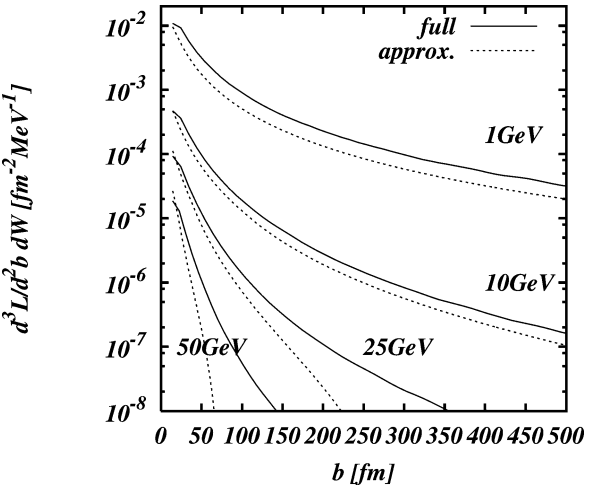

Fig. 6. The photon–photon luminosity $d^3L/d^2b\,dW$ is shown for different values of W as a function of the impact parameter b. The results of a full calculation for lead beams at the LHC are compared with the approximate result of Eq. (54).

GDR excitation is another example; the neutron transverse momentum tends to follow the electric field. The amplitude $a_{1,2}(\vec{b})$ for mutual excitation is

$$a_{1,2}(\vec{b}) = a_1(\vec{b})a_2(\vec{b}),$$

where the amplitude for single GDR excitation a_i $(i = 1, 2)$ is given, e.g., by Eq. (3.1.22) of [1].

In intermediate energy heavy-ion scattering (in contrast to the ultrarelativistic case) it is experimentally possible to measure directly the momentum transferred to the projectile. This determines the impact parameter vector $\vec{b}$. The decay products show a dependence on the azimuthal angle ϕ. This dependence has been observed, e.g., in the breakup reaction $^{11}\mathrm{Be} + \mathrm{Pb} \to {}^{10}\mathrm{Be} + n + \mathrm{Pb}$ in [51], see their Fig. 3. The angular distribution follows a dipole distribution, see Eq. (3.1.22) in [1]. For large values of γ the $m = \pm 1$ components dominate and

$$a_i \sim \sin\theta\cos\phi, \tag{57}$$

where θ and ϕ are the polar and azimuthal angles of the emitted neutrons in the system of the nucleus.

For mutual GDR excitation, the direction of $\vec{b}$ is the same for both excitations, producing a correlation between the emission angles of θ_1, θ_2, ϕ_1, and ϕ_2 (in the system of the respective emitting nucleus). The correlation in the relative azimuthal angle $\Delta\phi = \phi_1 - \phi_2$ of the emitted neutrons is

$$C(\Delta\phi) = 1 + \frac{1}{2}\cos(2\Delta\phi). \tag{58}$$

This correlation is shown in Fig. 7. The neutrons from the GDR decays can be detected with zero degree calorimeters which are located downstream of the collision region at

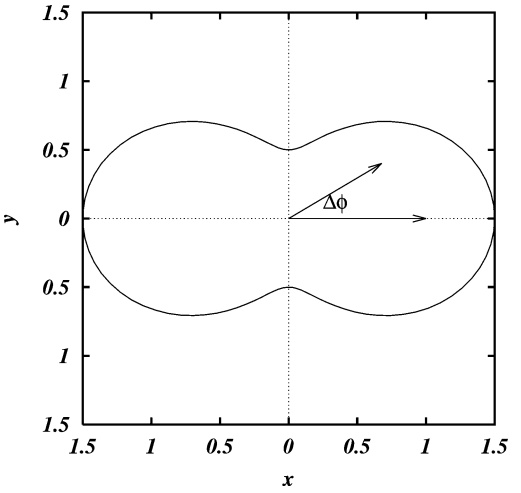

Fig. 7. The angular correlation of two neutrons emitted after mutual GDR excitation is shown. $\Delta\phi$ denotes the azimuthal angle between the two neutrons.

relativistic ion colliders. At RHIC, the ZDC's are located ± 18 meters downstream; they are 10 cm wide by 18.75 cm high [52]. The dimensions are limited by the available space. Although the sensitivity is reduced near the edges due to transverse shower leakage, coverage is good for angles $\theta < 2$ mrad [5]. The excitation energy for a heavy nucleus GDR is approximately 10 MeV, corresponding to a neutron momentum of about 140 MeV/c.

For the RHIC neutron longitudinal momentum of 100 GeV, $p_T = 140$ MeV/c corresponds to a deflection of 2.5 cm, well within the ZDC acceptance. With position sensitive shower-maximum detectors to the ZDC's, neutron position resolution of order 1 mm should be achievable [53], giving adequate angular resolution to study neutron–neutron correlations between the ZDCs. At the LHC, the ZDCs are located ± 116 meters from the collision regions, giving a maximum neutron deflection of 5 mm, so determining the neutron angular direction may be more difficult.

Similar angular correlations will occur for ρ production and decay to $\pi^+\pi^-$ accompanied by single or mutual GDR excitation. In its rest frame the ρ decay angular distribution is given by $|Y_{1M}(\theta, \Phi)|^2$, where M denotes the magnetic quantum number. The population of the different M-substates depends on the dynamics of the production process.

In the heavy-ion case the population is relatively simple, since the photons are almost real, with both helicities equally populated. It is the simplest assumption that in ρ photoproduction the ρ has the same polarization as the initial state photon—this is s-channel helicity conservation (SCHC). This has been experimentally verified for photoproduction [54,55] and for electroproduction [56]. In our case the photons are linearly polarized, transverse to the beam. Assuming SCHC, the final ρ^0 state is also linearly polarized, in the same direction as the equivalent photon. It is a superposition of $M = \pm 1$ states. The angular distribution in the rest system is

$$Y_{11} \pm Y_{1-1} = -\sqrt{\frac{3}{\pi}} \begin{cases} \sin\theta \cos\Phi, \\ i \sin\theta \sin\Phi, \end{cases} \tag{59}$$

quite analogous to Eq. (57) for the GDR decay. For exclusive ρ production, the direction of the impact parameter is unknown, and one has to integrate over all impact parameters. However, if the coherent ρ-production is accompanied by a GDR excitation, the azimuthal angles of the neutron and the $\pi^+\pi^-$-pair would be correlated, as with mutual GDR excitation. The GDR decay provides a way to measure the photon polarization. The same correlation would be observed between two ρ^0 that are produced together [12].

In e^+e^--pair production one also expects a dependence on the azimuthal angle ϕ which is defined by the impact parameter vector $\vec{b}$. For polarized (real) photons this can be seen from the analysis of, e.g., [57]. For linearly polarized photons the electron is most likely to be emitted in the plane of the polarization [57]. It will be of interest to do such theoretical calculations in more detail and work on this is currently in progress. E.g., in two-pair production one might expect to see such correlations, which leave their trace on the impact parameter of the collision. The formula for one-pair production in lowest-order semiclassical approximation is given, e.g., in [10,25,58]. This formula contains the correlations of the impact parameter and the momenta of the outgoing e^+e^--pair.

We conclude this section with a general remark on multi-photon processes. The observation of two electromagnetic processes with photon energies ω_1 and ω_2 gives information about the range of impact parameters of the collision. One has

$$P_{12}(b) = P_1(b)P_2(b) = N(\omega_1, b)N(\omega_2, b)\sigma_\gamma(\omega_1)\sigma_\gamma(\omega_2). \tag{60}$$

We use a simple approximation for the b-dependent equivalent photon spectrum $N(\omega, b)$:

$$N(\omega, b) = \frac{Z_1^2\alpha}{\pi^2 b^2} \quad \text{for } 2R < b < \frac{\gamma}{\omega}. \tag{61}$$

Thus such an interaction takes place in the b-range of $2R < b < \gamma/\omega_{\max}$, where $\omega_{\max}$ is the larger of ω_1 and ω_2.

4. Conclusions

Due to the strong fields of highly charged ions multi-photon processes are abundant in UPCs. The important modes were identified. Quite generally, the excitation of the different modes occurs independently and the corresponding amplitudes can be factorized. They do not influence each other. This is essentially due to the very high energy of the heavy ions, which is much higher than the energy ω of the equivalent photon. Only a small fraction of the total kinetic energy of the nuclei is lost in the UPC. Due to the coherence condition one has $x_{\max} = \omega/E = 1/(RM_NA) = \lambda_C(A)/R \ll 1$. M_N is the nucleon mass, and $\lambda_C(A)$ is the Compton wavelength of the nucleus.

The main result of this paper may seem intuitively obvious. However, the experimental implications are significant. The factorization assumption was used in detailed theoretical calculations of ρ-production and GDR excitation in [59] (following Table 2 it is said there that "the validity of the assumption of factorization is hard to prove rigorously..."), and [46], and in the corresponding experimental analysis [7]. It is important to show also how this factorization arises in the theoretical formulation of the process. Now there is a formal basis to discuss these questions theoretically.

Ultraperipheral heavy-ion collisions provide a strong source of equivalent photons up to very high energies. This offers the unique possibility to study photon–hadron (nucleus) and photon–photon processes in hitherto inaccessible regions, see [2]. Many UPC processes like GDR excitation are now recognized as useful for practical matters like luminosity measurement and impact-parameter dependent triggers. In this case, as was already shown explicitly in [46] one emphasizes the hard part of the spectrum, due to the selection of low b-values.

Acknowledgements

This work was partially supported by the US Department of Energy, under Contract No. DE-AC-03076SF00098. We would like to thank Sebastian White for interesting discussions on this subject. We thank also the Institute for Nuclear Theory at the University of Washington for its hospitality and the Department of Energy for partial support and the organizers of the program "The first three years of heavy ion physics at RHIC". The "UPC week" of this program, which took place 21–27 April 2003, was vital for this paper, both due to the interaction of some of the present authors and also to the stimulating atmosphere created by all the participants.

References

[1] C.A. Bertulani, G. Baur, Phys. Rep. 163 (1988) 299.
[2] G. Baur, K. Hencken, D. Trautmann, S. Sadovsky, Y. Kharlov, Phys. Rep. 364 (2002) 359.
[3] F. Krauss, M. Greiner, G. Soff, Prog. Part. Nucl. Phys. 39 (1997) 503.
[4] G. Baur, C.A. Bertulani, Phys. Lett. B 174 (1986) 23.
[5] M. Chiu, et al., Phys. Rev. Lett. 89 (2002) 012302.
[6] A. Baltz, C. Chasman, S.N. White, Nucl. Instrum. Methods 417 (1998) 1.
[7] C. Adler, et al., Phys. Rev. Lett. 89 (2002) 272302.
[8] H. Emling, Prog. Part. Nucl. Phys. 33 (1994) 729;
T. Aumann, P.F. Bortignon, H. Emling, Annu. Rev. Nucl. Part. Sci. 48 (1998) 351.
[9] K. Hencken, D. Trautmann, G. Baur, Phys. Rev. A 51 (1995) 998.
[10] K. Hencken, D. Trautmann, G. Baur, Phys. Rev. A 51 (1995) 1874.
[11] A. Aste, G. Baur, K. Hencken, D. Trautmann, G. Scharf, Eur. Phys. J. C 23 (2002) 545.
[12] S. Klein, J. Nystrand, Phys. Rev. C 60 (1999) 014903.
[13] G. Baur, in: W. Marciano, S. White (Eds.), Proceedings of the Workshop on Electromagnetic Probes of Fundamental Physics, Erice, Italy, October 16–21, 2001, World Scientific, Singapore, 2003, p. 183, hep-ph/0112239.
[14] J.D. Jackson, Classical Electrodynamics, 2nd Edition, Wiley, New York, 1975.
[15] M. Levy, J. Sucher, Phys. Rev. 186 (1969) 1656.
[16] G. Tiktopolous, S.B. Treiman, Phys. Rev. D 2 (1970) 805.
[17] F. Hayot, C. Itzykson, Phys. Lett. B 39 (1972) 521.
[18] E. Fermi, Z. Phys. 29 (1924) 315.
[19] E. Bartos, et al., Phys. Lett. B 538 (2002) 45.
[20] P.M. Morse, H. Feshbach, Methods of Theoretical Physics, McGraw–Hill, New York, 1953.
[21] C.A. Bertulani, C.M. Campbell, T. Glasmacher, CPC 152 (2003) 317.
[22] W.E. Frahn, Ann. Phys. (N.Y.) 72 (1972) 524.
[23] W. Nörenberg, H.A. Weidenmüller, Introduction to the Theory of Heavy-Ion Collisions, 2nd Enlarged Edition, Springer-Verlag, Berlin, 1980.

[24] K. Alder, A. Bohr, T. Huus, B. Mottelson, A. Winther, Rev. Mod. Phys. 28 (1956) 432.
[25] L.D. Landau, E.M. Lifschitz, Lehrbuch der Theoretischen Physik, Vol. 4, Akademie-Verlag, Berlin, 1986.
[26] G. Baur, Z. Phys. A 332 (1989) 203.
[27] K. Hencken, D. Trautmann, G. Baur, Z. Phys. C 68 (1995) 473.
[28] K. Hencken, D. Trautmann, G. Baur, Phys. Rev. C 53 (1996) 2532.
[29] F. Meissner, V. Morozov, nucl-ex/0307006.
[30] G. Baur, Nucl. Phys. A 531 (1991) 685.
[31] S. Klein, R. Vogt, Phys. Rev. C 68 (2003) 017902.
[32] K. Alder, A. Winther, Electromagnetic Excitation: Theory of Coulomb Excitation with Heavy Ions, North-Holland, Amsterdam, 1975.
[33] E. Merzbacher, Quantum Mechanics, 2nd Edition, Wiley, New York, 1970.
[34] R. Glauber, Phys. Rev. 131 (1963) 2766.
[35] J.R. Klauder, B.-S. Skagerstam, Coherent states, World Scientific, Singapore, 1985.
[36] G. Baur, C.A. Bertulani, Nucl. Phys. A 482 (1988) 313c.
[37] C.A. Bertulani, in: W. Marciano, S. White (Eds.), Proceedings of the Workshop on Electromagnetic Probes of Fundamental Physics, Erice, Italy, October 16–21, 2001, World Scientific, Singapore, 2003, p. 203, nucl-th/0201060.
[38] G. Baur, C.A. Bertulani, in: R.A. Broglia, G. Bertsch (Eds.), Proceedings of International School of Heavy Ion Physics, October 12–22, 1986, Erice, Italy, Plenum Press, New York, 1988, p. 343.
[39] I.A. Pshenichnov, I.N. Mishustin, J.P. Bondorf, A.S. Botvina, A.S. Ilinov, Phys. Rev. C 57 (1998) 1920.
[40] I.A. Pshenichnov, J.P. Bondorf, I.N. Mishustin, A. Ventura, S. Masetti, Phys. Rev. C 64 (2001) 024903.
[41] G. Baur, Phys. Rev. A 42 (1990) 5736.
[42] R.N. Lee, A.I. Milstein, V.G. Serbo, Phys. Rev. A 65 (2002) 022102.
[43] K. Hencken, Yu. Kharlov, S. Sadovsky, Generator of e^+e^--pairs in PbPb collisions at LHC, ALICE Internal Note ALICE-INT-2002-27, 2002.
[44] K. Hencken, Yu. Kharlov, S. Sadovsky, Ultraperipheral trigger in ALICE, ALICE Internal Note ALICE-INT-2002-11, 2002.
[45] A.G. Shamov, V.I. Telnov, Nucl. Instrum. Methods A 494 (2002) 51.
[46] A.J. Baltz, S.R. Klein, J. Nystrand, Phys. Rev. Lett. 89 (2002) 012301.
[47] S.R. Klein, J. Nystrand, Phys. Rev. Lett. 84 (2000) 2330.
[48] H.A. Bethe, R.W. Jackiw, Intermediate Quantum Mechanics, Benjamin, New York, 1968.
[49] M. Abramowitz, I.A. Stegun, Handbook of Mathematical Functions, National Bureau of Standards, Washington, DC, 1964.
[50] S. Klein, Transparencies of the second UPC workshop, Geneva, October 11–12, 2002, available at http://quasar.unibas.ch/UPC/.
[51] T. Nakamura, et al., Phys. Lett. B 331 (1994) 296.
[52] C. Adler, et al., Nucl. Instrum. Methods A 470 (2001) 488.
[53] S. White, personal communication, May 2003.
[54] L. Criegee, et al., Phys. Rev. Lett. 25 (1970) 1306.
[55] J. Ballam, et al., Phys. Rev. D 7 (1973) 3150.
[56] J.A. Crittenden, Exclusive production of neutral vector mesons at the electron–proton collider HERA, in: Springer Tracts in Modern Physics, Vol. 140, Springer, Heidelberg, 1997.
[57] W.H. McMaster, Rev. Mod. Phys. 33 (1961) 8.
[58] A. Alscher, K. Hencken, D. Trautmann, G. Baur, Phys. Rev. A 55 (1997) 55.
[59] A.J. Baltz, S.R. Klein, J. Nystrand, nucl-th/0203062.